Saturated Absorption Spectroscopy of Molecular Iodine for Laser Locking

Tony Metger
Supervisor: Christoph Fischer

July 27, 2017

Abstract

Locking a laser to an atomic transition ensures a stable and precisely known laser frequency. In this work saturated absorption spectroscopy is performed on molecular iodine. In a similar setup an error signal was obtained by processing the spectroscopic signal using a lock-in-amplifier. Here, an alternative method without the use of a lock-in-amplifier is presented. Based on the work of M. Aldous et al. [5], two collinear beams at frequencies differing by 8 MHz are used for saturated absorption spectroscopy, with the difference signal being suitable as an error signal without further processing. A laser at a wavelength of approximately 570.7 nm was locked to a hyperfine feature of the R115 (20-1) absorption line of molecular iodine. The lock proved to be very stable under the influence of external perturbations. The frequency doubled output of this laser will be used for addressing the ${}^1S_0 \rightarrow {}^1P_1$ transition in neutral magnesium.

Contents

1 Introduction

A laser can be locked to a spectroscopic line of an atom or molecule, meaning that the frequency of the laser light is controlled in such a way that it is equal to the frequency of this spectroscopic line and does not drift over time. The thermal motion of the atoms on which spectroscopy is performed causes a Doppler shift in the frequency of light able to excite a transition. Because the directions of velocity vectors are randomly distributed inside a gas, the spectral lines are Doppler broadened (section 2.2 and [1, pp. 151-153]). To resolve the underlying atomic structure of thermal atoms, saturated absorption spectroscopy can be performed (section 2.3 and [2]).

To lock the laser, an error signal proportional to the frequency offset of the laser from the desired frequency is needed. This error signal can be generated by taking the derivative (or an approximation thereof) of the saturated absorption spectrum. In a similar setup [3, section 5.4] [4, section B], this was done using a lock-in amplifier. Another approach for converting the spectroscopic signal to an error signal is to use two beams at different frequencies to obtain a finite-difference approximation of the derivative [5]. This approach (referred to in the following as the double-beam method) is the one used here to lock a laser to a hyperfine iodine transition.

In the following, section 2 provides theoretical background on laser locking, Doppler broadening, saturated absorption spectroscopy and the double-beam method. Section 3 describes the experimental implementation of the double-beam method and gives details on pitfalls. Results from the presented setup, in particular the stability of the lock, are shown in section 4. The appendix contains a number of theoretical derivations as well as recommended settings for the presented setup.

2 Theoretical Background

2.1 Laser Locking

The frequency of a laser can naturally drift due to a variety of factors such as changes in temperature or pressure causing the length of the optical cavity to change. Many lasers use electronic systems to actively counteract this drift. These systems need an error signal as input, which gives an indication of the difference between the actual and desired frequency of the laser.

The electronic system used to lock the laser always works to minimize the error signal fed to it. Therefore, at the desired frequency of the laser, the error signal must be zero, whereas for frequencies differing from the set point, the error signal should be proportional to the frequency offset, which allows the system to change the frequency more when the laser is far from the desired frequency and less when it is already close. This avoids overcorrecting, which would result in an oscillating laser frequency. Thus, the ideal error signal is linear with a zero-crossing at the desired frequency.

More realistically, the error signal might be linear for some interval, as shown in Fig. 2.1. The frequency interval for which the error signal is linear should be such that one expects to never find the laser frequency outside this interval, i.e. the locking system has to work quickly enough to always keep the laser frequency inside this interval even when the laser experiences external perturbations (such as people walking by, someone hitting the case of the laser, etc.). If the laser frequency does move outside this interval, the locking system can no longer work properly and the laser will in general not return

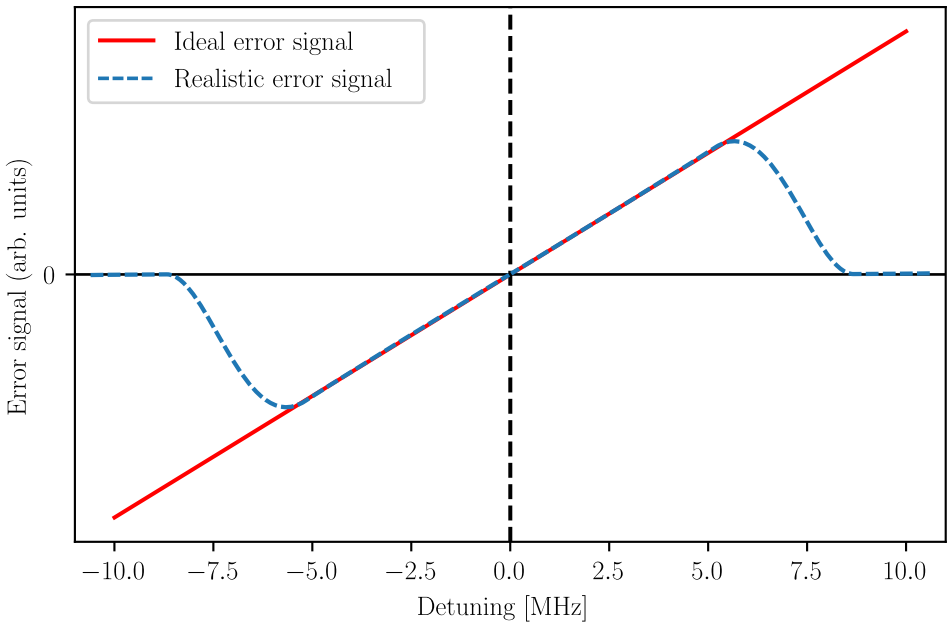

Figure 2.1: Desired shape of the error signal. The ideal error signal would be a linear function (red). Realistically, this can only be achieved in some frequency interval (blue). The values on the x-axis only serve to provide an idea of the orders of magnitude involved.

to the desired frequency. This is referred to as the laser jumping out of lock. [6]

To obtain an error signal such as the one shown in Fig. 2.1, it is necessary to have a frequency reference which is not dependent on the same environmental factors as the laser frequency. Commonly, hyperfine transitions in atoms or molecules are used for this purpose, since the frequency of light emitted by such a transition depends only on the atomic energy level structure.

The saturated absorption signal of such a hyperfine transition (see section 2.3) has a Lorentzian lineshape and its height depends on the intensity of the laser, making it less suitable as an error signal[1]. To get the desired linear error signal, one can take the derivative of the saturated absorption signal. Because a peak behaves approximately like a quadratic function on some interval, this will yield a linear dependence of the signal on the frequency offset with a zero-crossing at the position of the maximum, i.e. the position of the desired frequency.

The error signal can be fed to a proportional-integral-controller (PI controller), the output of which is used to adjust the current through the laser diode, which changes the frequency of the laser.

[1]To use the unprocessed saturated absorption signal as an error signal, one could think of tuning the laser to the half-maximum point and monitoring the fluorescence. A change of the laser's frequency would lead to either a linear increase or decrease in fluorescence, depending on the direction of the frequency drift. However, an increase or decrease in laser power would have the same effect. Therefore, it is advantageous to have an error signal which does not depend on the laser's intensity.

2.2 Doppler Broadening

Doppler broadening refers to the broadening of spectral lines due to the thermal motion of the atoms in a gas and the resulting Doppler shift of the light that is absorbed or emitted ([1, section 8.1]).

Because the atoms in a gas move with velocities on the order of 10^2 m/s ([7, section 4.7.6]), the light frequency which they can absorb light is shifted due to the Doppler effect to

$$f' = f_0(1 - v/c)\,,$$

where f_0 is the transition frequency and v is the velocity with which the atom moves in the direction of the beam impinging on it [8, chapter 15]. For example, for a spectroscopic line at 568 nm and an atom moving with 100 m/s, the frequency is shifted by approximately 180 MHz.

Since the direction in which atoms move is randomly distributed, different atoms with identical transition frequencies will absorb light at different frequencies depending on their velocity. Therefore, the absorption spectrum does not display a sharp line at f_0, but instead a broadened peak around f_0. The shape of this peak is derived in appendix A and turns out to be a Gaussian with standard deviation $\sigma_{\text{Doppler}} = \sqrt{\frac{kT}{m}}\frac{f_0}{c}$, where k is the Boltzmann constant, T the temperature, m the molecular mass and c the speed of light.

2.3 Saturated Absorption Spectroscopy

Saturated absorption spectroscopy (also referred to as Doppler-free spectroscopy) is a spectroscopic method that achieves much higher resolution compared to standard (Doppler broadened) spectroscopy by using the fact that two beams impinging on an atom from opposite sides are Doppler-shifted in opposite directions in the rest frame of the atom [2].

Specifically, two overlapping beams of differing intensity travelling in opposite directions are passed through a gas cell. The stronger pump beam is absorbed by atoms with a velocity v (along the direction of the beam), whereas the weaker probe beam is absorbed by atoms with velocity $-v$. Both pump and probe beam have the same frequency f_L. An atom needs to have velocity $v = c(f_0 - f_L)/f_0$ to absorb light with frequency f_L, and all atoms with velocity v (or very close to v) are said to belong to the velocity class v. A sufficiently strong pump beam will deplete the ground state population of the velocity class v, i.e. the absorption will saturate. As one scans the frequency of the laser, different velocity classes will be saturated.

The velocity class v saturated by the pump beam and the velocity class $-v$ absorbing the probe beam will coincide if and only if $v = 0$, which is the case if and only if $f_L = f_0$. In this case, the absorption of the probe beam will decrease, as the velocity class the probe beam is absorbed by has already been saturated by the pump beam. Thus, as one scans the frequency of the laser, one will observe a bump in the intensity of the probe beam at $f_L = f_0$ (see Fig. 4.1). This bump is much narrower than the Doppler broadened line, because only atoms of one velocity class ($v = 0$) are involved.

By subtracting the probe beam signal from a Doppler-broadened absorption signal (commonly obtained by passing a reference beam through the probe which does not overlap with the pump beam), one gets a saturated absorption spectrum. In this spectrum, hyperfine peaks are usually resolved. As an example, the hyperfine spectrum

of the 568.2 nm line of molecular iodine obtained from such a probe-reference setup is shown in Fig. 2.2.

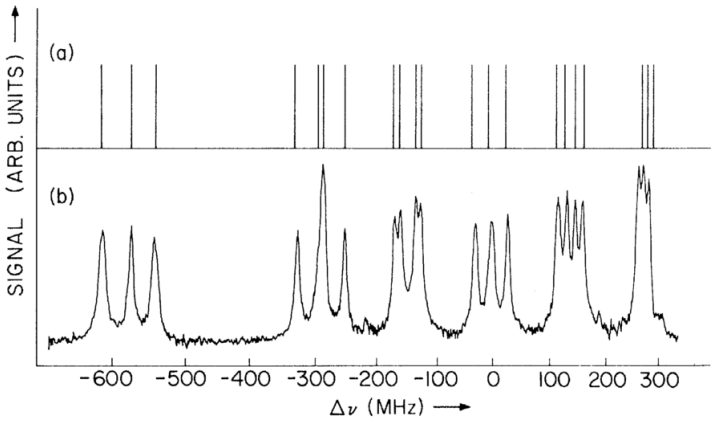

Figure 2.2: Hyperfine spectrum of 568.2 nm iodine line. (a) shows the theoretical positions of the transitions, whereas (b) displays the spectrum measured using saturated absorption spectroscopy. Almost all hyperfine lines are resolved. The figure is taken from [9].

2.4 Double-Beam Method

As described in section 2.1, the derivative of a saturated absorption spectrum has to be taken to get an error signal. The double-beam method described here uses two parallel saturated absorption setups at slightly different frequencies to obtain a finite-difference approximation of the derivative [5].

In the double-beam method, two beams at frequencies $f_L \pm f_{\text{mod}}$ are produced using an acousto-optic modulator (AOM) driven with two frequencies $f_C \pm f_{\text{mod}}$. Because the angle at which a diffracted beam leaves an AOM depends on the AOM frequency, this produces two diffraction patterns at slightly different angles. The first diffraction order of each pattern is used for two parallel saturated absorption setups, which yield two identical spectra shifted with respect to each other by $2f_{\text{mod}}$. Subtracting these two spectra from each other gives an approximation of the derivative of the unshifted spectrum as a function of the laser frequency f_L, since for a signal $s(f_L)$:

$$s'(f_L) \approx \frac{s(f_L + f_{\text{mod}}) - s(f_L - f_{\text{mod}})}{2f_{\text{mod}}}$$
$$\implies s(f_L + f_{\text{mod}}) - s(f_L - f_{\text{mod}}) \approx 2f_{\text{mod}} s'(f_L)\,.$$

In practice, $f_{\text{mod}} \approx f_{\text{HWHM}}$ where f_{HWHM} is the half width at half maximum of the saturated absorption peak, because otherwise the two beams do not diverge enough to be separable and the difference signal is too small. Then, the difference signal more closely resembles the juxtaposition of a peak and a dip, but still has the desired form (see Fig. 2.3 and compare with Fig. 2.1).

3 Experimental Implementation

The double-beam method described in section 2.4 was used to lock a laser to a hyperfine transition in molecular iodine. Here, details of the experimental setup as well as failed

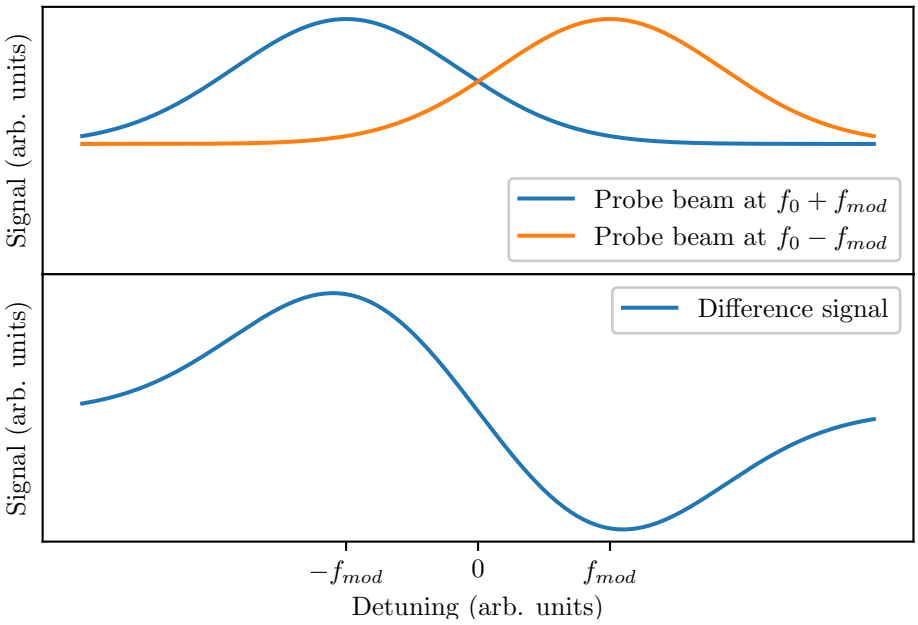

Figure 2.3: Illustration of the error signal from the double-beam method. For $f_{\text{mod}} = f_{\text{HWHM}}$, the two saturated absorption peaks hardly overlap, but the difference signal still can be used as an error signal.

attempts and pitfalls are presented.

3.1 Current Experimental Setup

A schematic drawing of the setup is shown in Fig. 3.1. Throughout this section, labels from the drawing will be used to refer to individual components. A table summarizing recommended settings for the different electrical components can be found in appendix C.

The setup can be divided into four stages: single beam preparation (red background in Fig. 3.1), double beam preparation (blue background), saturated absorption spectroscopy (green background) and signal processing.

The entire setup as well as the laser it locks are housed in a closed shock-absorbing box to minimize noise from vibrations and air movement.

Single Beam Preparation

The first stage serves to control the intensity and frequency shift (relative to the laser frequency, see below) of the beam used for locking.

The linearly polarized beam coming from the laser (Toptica TA-FHG pro) with power $P = 20$ mW is first passed through a half-waveplate followed by a polarizing beam splitter (PBS1). By rotating the half-waveplate, one can rotate the polarization of the beam, which changes the intensity of the beam after PBS1. Usually, the intensity of the beam after PBS1 should be maximized, but a weaker beam may be useful for testing parts of the setup.

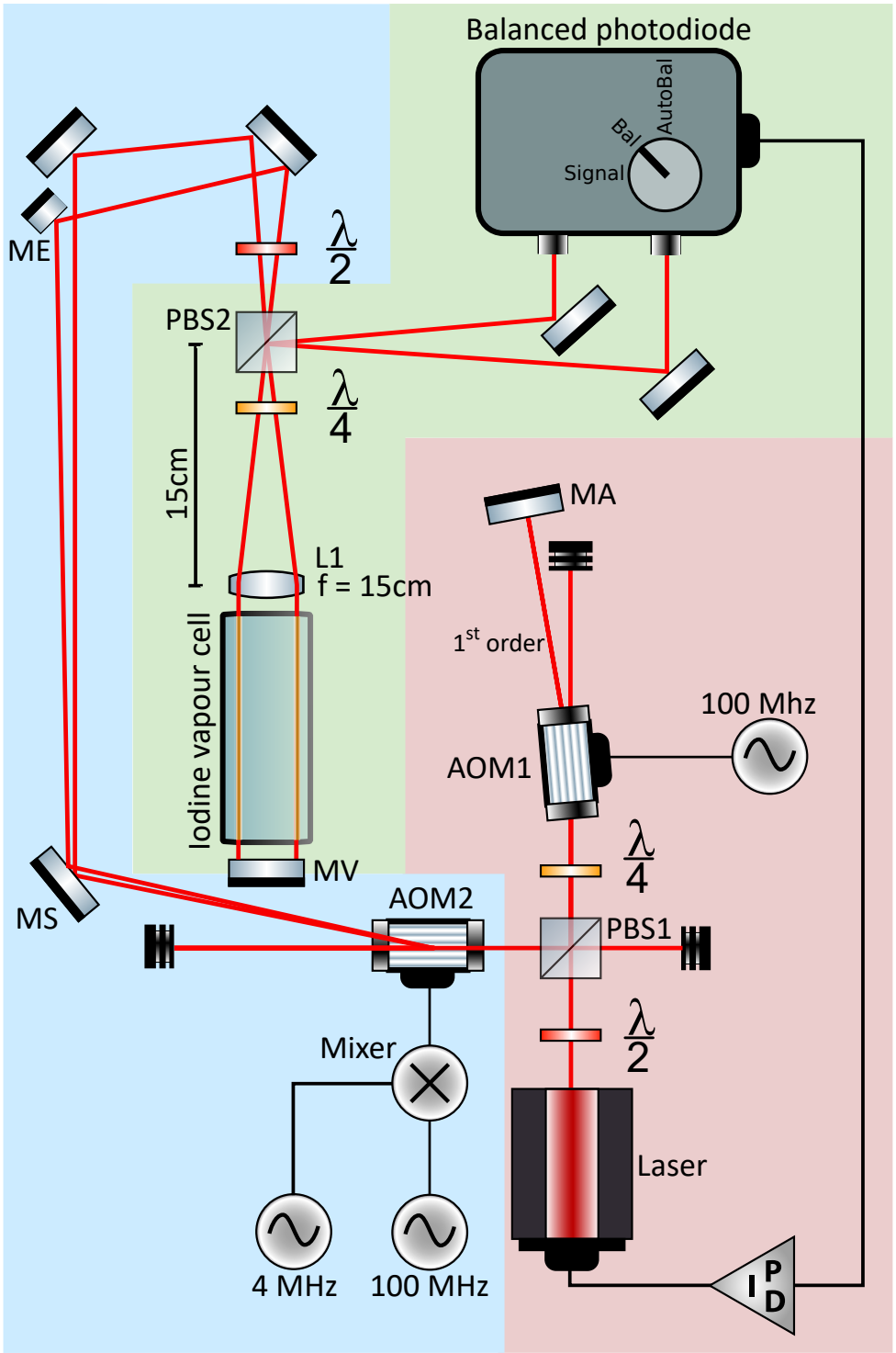

Figure 3.1: Schematic drawing of the setup. The experimental setup consists of three parts: Part 1 (red background in the figure) shifts the frequency of the laser light and controls its intensity. Part 2 (blue background) serves to create two beams at frequencies $f \pm f_{\text{mod}}$ with a large angular separation. Part 3 (green background) performs saturated absorption spectroscopy with both beams separately and creates the error signal by taking the difference between both signals using a balanced photodiode.

The light frequency needs to be shifted because the laser will be used to cool magnesium atoms, which requires a slightly different frequency than that of the hyperfine iodine transition used for locking. To this end, an acousto-optic modulator (AOM1) is passed twice, with the first diffraction order being picked off both times. In total, this shifts the frequency of the light by $2f_C$, where f_C is the carrier frequency of AOM1. Additionally, the beam passes a quarter-waveplate both before and after being reflected by mirror MA, which, in total, rotates the polarization by $\pi/2$. Hence, the beam is reflected on its way back by PBS1.

Double Beam Preparation

To implement the double-beam method (section 2.4), two spatially separated beams at frequencies $f_0 \pm f_{\mathrm{mod}}$, $f_{\mathrm{mod}} \ll f_0$ are needed. These are generated by passing the beam through AOM2 (AA Optoelectronics MT110-B50A 1,5-VIS) driven with two frequency tones $f_C \pm f_{\mathrm{mod}}$, which creates two diffraction patterns at slightly different angles. The signal used to drive the AOM is generated by applying the carrier tone f_C to the radio-frequency (rf) port and the modulation f_{mod} to the DC port of a radio-frequency-mixer (MiniCircuits ZX05-1L-S+).

The first diffraction orders of both diffraction patterns are spatially separated by passing a distance of approximately 60 cm. Then, an edge mirror ME is used to pick off one beam. This has two advantages over using a longer optical path for spatial separation: First, a longer optical path would increase the beam diameter and make the setup more susceptible to changes in air pressure. Secondly, using an edge mirror uncouples the separation distance and the beam diameter, which allows one to focus each beam individually without having them cross each other at the focal point. This is not possible without an edge mirror, because both the beam diameter and the separation increase linearly with the distance from AOM2. Thus, for any focusing lens, the focal point of the two beams is at the same position as their waists.

Note that by changing the azimuthal angle of MS one can easily control the position of the double-beam-spot at ME, which in turn determines how much power goes into each of the beams later passing the iodine cell.

Saturated Absorption Spectroscopy

The two spatially and angularly separated beams can be now be used to perform two parallel saturated absorption spectroscopy measurements.

The polarizing beam splitter PBS2 is placed such that the two beams separated at ME cross each other at its center. This placement is arbitrary, but provides a good visual reference for adjusting the position of lens L1. The half- and quarter-waveplate are used to control which beams pass and reflect off the PBS in a scheme identical to that described for the single beam preparation. Care has to be taken so that both beams fully pass through the small waveplates, which is why they are best placed close to PBS2, where beam separation is small.

Lens L1 (with focal length $f = 15$ cm) is used to make the two beams parallel and focus each one individually. The beam travelling from L1 through the iodine cell serves as the pump beam, whereas the beam travelling back after reflection at mirror MV is the probe beam.

It is critical that both beams are completely parallel after passing L1 to ensure good overlap of the pump and probe beam inside the iodine cell. L1 should therefore

be placed at distance f from the PBS, but its position has to be fine-tuned by both observing the beams inside the iodine cell as well as the saturated absorption signal from the detector.

Using an optical neutral density filter to weaken the probe beam turns out to be unnecessary and results in a worse signal-to-noise-ratio.[2]

The focal length of L1 and the position of MV are chosen such that both beams are focused on MV. This way the reflected probe beam has the same diameter as the pump beam throughout the iodine cell. To minimize the beam diameter inside the iodine cell, MV ought to be placed close to the iodine cell, and its angle must be adjusted for maximum overlap of pump and probe beam. It should be stressed that the quality of the error signal is extremely sensitive to the placement of L1 and the angle of MV, because if the two beams are not exactly parallel or reflected at an angle other than 90 degrees, the reflected probe beams will not perfectly overlap. The consequences of imperfect overlap are aggravated by the small diameter of pump and probe beam.

Finally, the beams are fed to the signal and reference sensor of the balanced photodiode (Newport Nirvana model 2007).

Signal Processing

The error signal from the photodiode is processed using a PI-controller and then fed back to the laser. The recommended P- and I-gains are listed in appendix C.

3.2 Failed Attempts and Pitfalls

Here, a number of failed attempts and pitfalls to watch out for are described. It may be useful to refer to this section when trouble-shooting a similar setup.

Large Beam Diameter

The beam diameter should be as small as possible, for otherwise the pump beam may not saturate the iodine. Experimentally, it was observed that a beam diameter of approximately 1 mm inside the iodine cell produces a saturated absorption signal. For a beam with a diameter of approximately 3 mm inside the iodine cell, only the Doppler signal was observed. To keep the beam diameter small, one should keep the path length between AOM2 and the iodine cell as small as possible (but long enough to be able to separate the two beams precisely) and use a lens such as L1 to focus the beams inside the iodine cell.

Beams Crossing in Iodine Cell

In an attempt to reduce the beam diameter inside the iodine cell, two lenses were used to focus the two beams to a common focal point as shown in Fig. 3.2. While this is very effective for obtaining a small beam diameter inside the iodine cell from two initially parallel beams and is much more insensitive to small changes in the positions of the

[2]When using a beam intensity that fully saturates the transition, the line width exhibits power broadening. In that case, an optical neutral density filter should be used to weaken the probe beam. With the beam intensity used in this experiment, power broadening is not a concern and thus an optical neutral density filter is unnecessary.

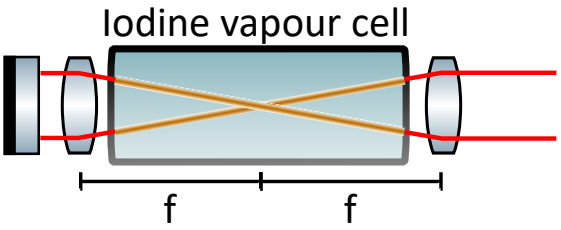

Figure 3.2: Crossing beams inside Iodine cell. This setup does not produce a usable error signal.

lenses than the setup described above, the resulting error signal has the following two undesirable properties:

1. Asymmetry: The height of the the peak at $f - f_{\text{mod}}$ and the dip at $f + f_{\text{mod}}$ differ, with one being up to 4 times the height of the other.

2. Dependence on scanning speed: The strength of the error signal depends on the scanning velocity (scanning range $\times$ scanning frequency), with a higher scanning velocity yielding a stronger signal.

These two properties render the error signal useless for locking. Especially the dependence on scanning speed is expected to make locking impossible. A slow drift in frequency corresponds to a scanning speed of almost zero. Because the error signal tends to zero for small scanning velocities the controller will not notice when the laser is slowly drifting away from its lock point.

In appendix B, a qualitative explanation is given for why crossing beams cause the error signal to degrade, but the specific effects observed in the experiment could not be reproduced theoretically.

Beam Alignment

Saturated absorption spectroscopy is conditioned on the pump and probe beam overlapping, since otherwise the velocity-dependent ground state depletion described in section 2.3 does not affect the probe beam. Therefore, it is necessary to ensure excellent beam alignment inside the iodine cell. For this, L1 has to be placed such that the two beams passing through the cell are perfectly parallel, as otherwise the reflected probe beams cannot fully overlap with their respective pump beams for the entire length of the iodine cell. Similarly, MV has to be adjusted for maximum overlap. Coarse adjustment of beam alignment can be done by eye, whereas for fine adjustment it is recommended to observe the photodiode signal and maximize the size of the saturated absorption bumps in the spectrum with the photodiode on the "Signal" setting.

Differing Beam Intensity

If the intensities of the two beams differ, the difference signal is offset from 0 and, more problematically, asymmetric. Therefore, care has to be taken to ensure both beams are of the same intensity. This is best done by changing the angle of mirror MS until the balanced signal (not auto-balanced) of the photodiode is centred around 0.

Unstable AOMs

The AOMs (especially AOM2) need about 10-20 minutes to warm up. During this time, the signal is very unstable.

Low-Sensitivity Photodiode

The photodiode has to be sensitive enough to detect the saturated absorption bumps. For example, a Thorlabs PDQ80A photodiode proved to be too noisy for this application.

Auto-Balanced Photodiode

The "Autobalance" and "10x" settings on the Newport Nirvana photodiode do not work for locking the laser. The reason for this is that the auto-balancing is achieved by high-pass filtering the signal. Hence a slowly varying DC signal below the cutoff frequency of the high pass filter cannot be seen. In a similar setup [3] the signal is modulated at a frequency of 15 kHz and therefore can be auto-balanced with correct filter settings. These settings (especially the "10x" setting) can however be useful for observing the error signal and fine-tuning the beam alignment inside the iodine cell.

4 Results

4.1 Single-Beam Saturated Absorption Signal

A scan of the saturated absorption signal of a single beam (i.e. a measurement of the signal as a function of the frequency detuning) is shown in Fig. 4.1. As expected, bumps in the broad Doppler spectrum are visible. However, the bumps are not very pronounced, hinting at the fact that the iodine might not be fully saturated in a sufficiently large region.

Unlike in the theoretical model (section 2.3, appendix B.1), a bump does not always occur at the minimum of the Doppler broadened absorption spectrum. This is due to the fact that the Doppler broadened spectrum measured by the photodiode is the superposition of the Doppler-broadened spectra of all hyperfine iodine lines making up a single gross structure line. Therefore, a bump produced by one of the off-center hyperfine lines (which can be resolved with saturated absorption spectroscopy) will not lie at the center of the cumulative Doppler broadened spectrum.

4.2 Scan of Error Signal

The error signal can be scanned to gauge its quality and suitability for locking. Ideally, one would like to obtain a signal such as the one shown Fig. 2.1.

The signal produced by the double-beam setup with a modulation frequency $f_{\text{mod}} = 4$ Mhz is shown in Fig. 4.2 and is indeed very similar to the ideal form. In particular, the signal is symmetric and linear in an interval of length almost $2f_{\text{mod}}$.

Note that unlike the single-beam signal in Fig. 4.1, the error signal is not averaged. A non-averaged single beam signal has a very poor signal-to-noise ratio (about 1:1 or 2:1), whereas the averaged error signal is of much higher quality. This is becuase the subtraction of the two signals cancels out noise common to both. This cancellation of

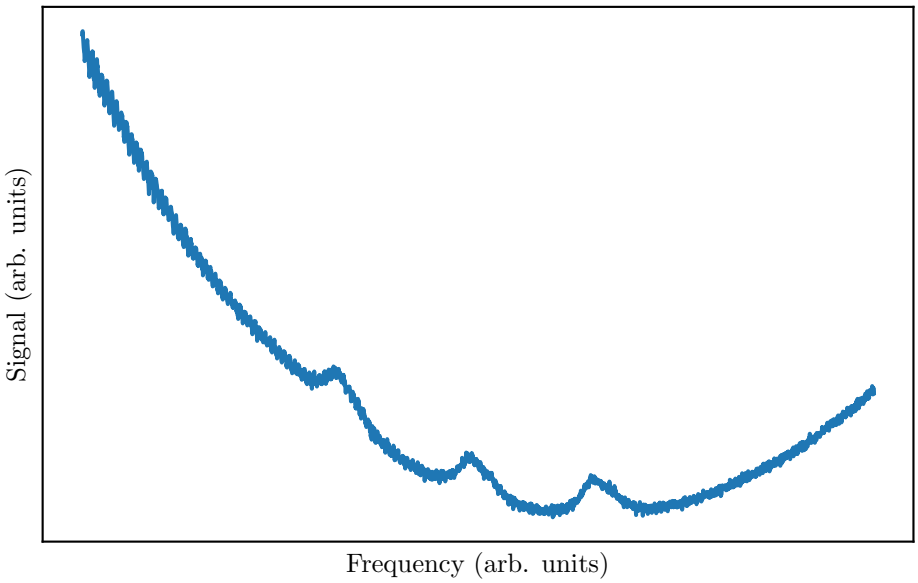

Figure 4.1: Single-beam spectrum. The single-beam signal (averaged over 128 periods) shows the expected bumps overlaid onto a broad Doppler spectrum.

noise does not occur in a setup using a single beam with a lock-in amplifier and presents a significant advantage [3] [4].

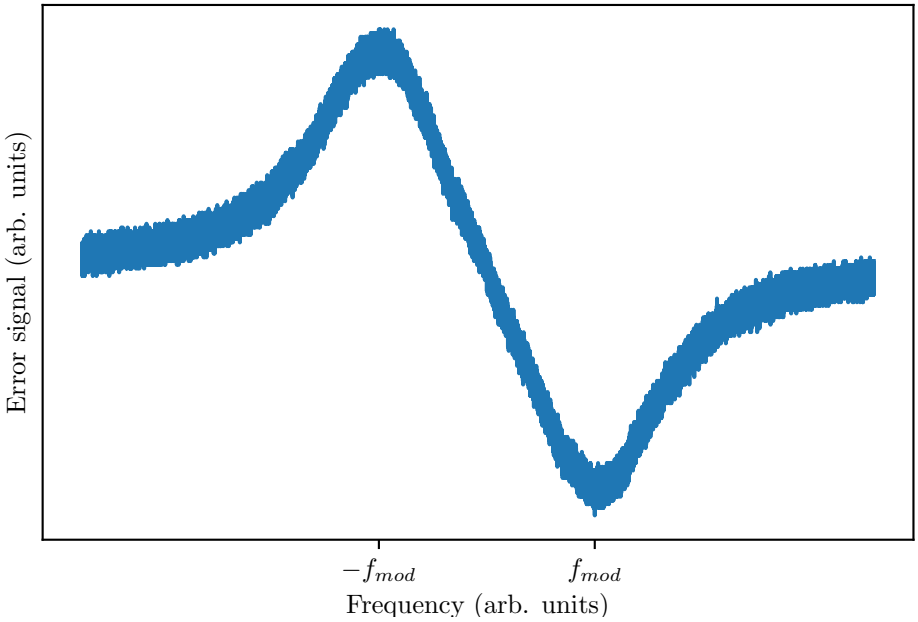

Figure 4.2: Double-beam error signal for $f_{\text{mod}} = 4$ Mhz. The error signal as a function of frequency detuning is of the desired form. For frequency detuning between $-f_{\text{mod}}$ and $+f_{\text{mod}}$, the signal is almost linear.

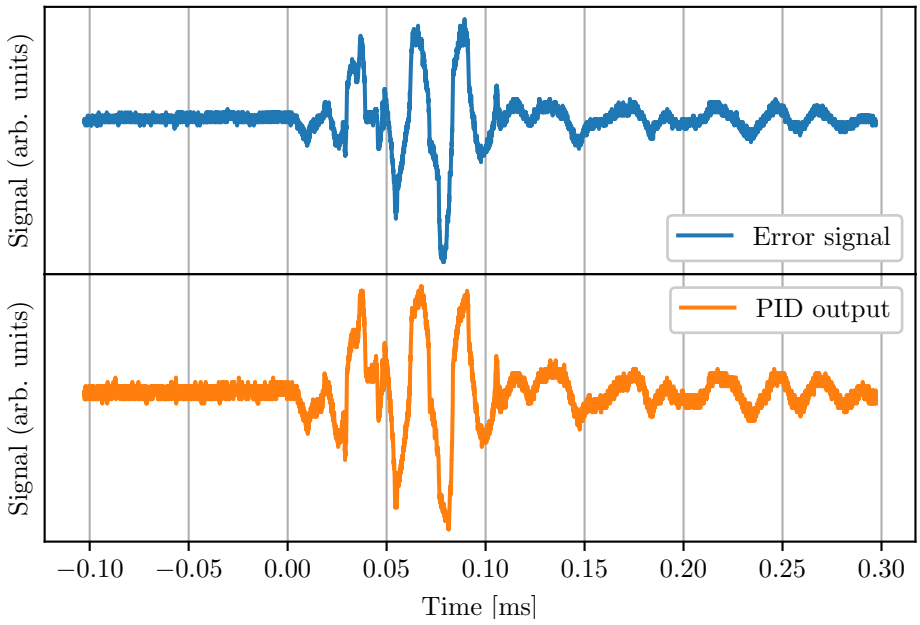

Figure 4.3: Error signal and PI output after external perturbation. The box in which laser and locking setup are housed is hit at $t = 0$. The oscillations of the error signal are matched closely by the PI output and the laser stays locked.

4.3 Stability of the Lock

The laser typically stays locked for times on the order of 30 min to 1 hour. This is achieved only when both the laser and the double-beam setup are housed in the same closed, shock-absorbing box.

Response to External Perturbations

The lock is remarkably stable when subjected to external perturbations (e.g. the box in which the lock is housed is hit).

Fig. 4.3 shows the error signal as well as the PI output after such an external perturbation. The box in which the lock and laser are housed is hit at $t = 0$. One can see the lock working well, with the output following the form of the error signal very closely and almost without time delay. The error signal and the PI output return to their initial values for large t, so the laser stays locked to the selected hyperfine transition. Checking the frequency by switching back to scanning mode on the PI controller confirms that the laser stayed locked.

Characterization of Unlock Events

Two different types of unlock events were observed: On the one hand, an unlock event can occur under the influence of external perturbations. On the other hand, the laser can slowly drift out of lock over time-scales of several seconds. In day-to-day operation, the second type seems to be more common, especially since the lock-setup and laser are housed in a shock-absorbing box.

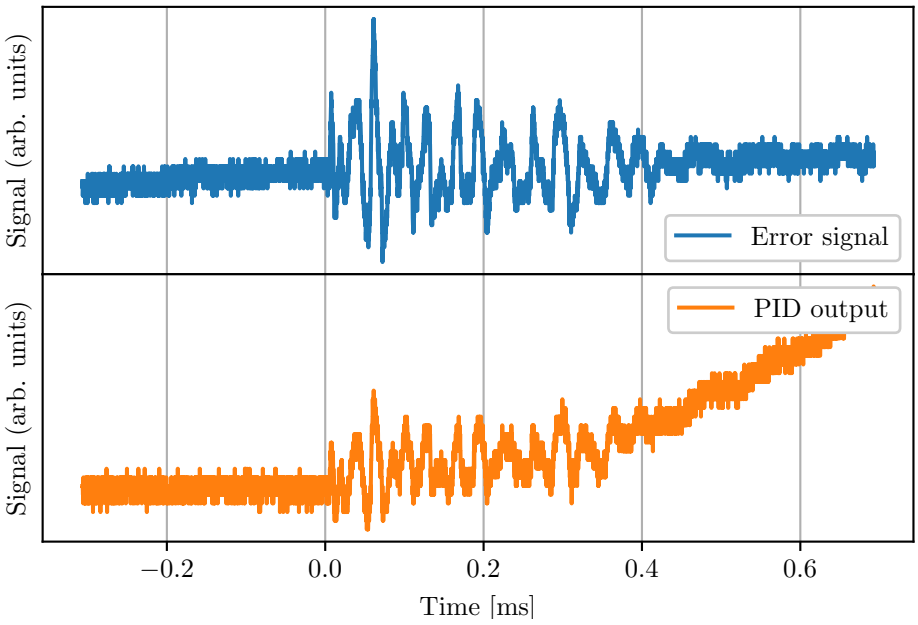

Figure 4.4: External perturbation leading to unlock event. Initially, the PI output responds well to the spikes in the error signal due to an external perturbation at time $t = 0$. However, the PI output is not symmetric around 0. Therefore, the integral term in the PI-amplification causes the output to grow without bounds once the error signal has returned to a constant value.

When an external perturbation causes spikes in the error signal, the lock usually responds well and returns the laser to its previous locked state as described above. However, in some cases, the system does not work properly, an example of which is shown in Fig. 4.4. Initially, the PI output matches the error signal closely. At time $t = 0.06$ ms, the output seems to fail to respond adequately, since the relative size of the spike at $t = 0.06$ ms compared to other spikes is smaller in the output than in the error signal. For times $t > 0.06$ ms, the output still has the same form as the error signal, so the laser frequency has not left the part of the error signal which displays linear behaviour (as explained in section 2.1). However, the offset of the PI output is shifted (i.e. the PI controller returns a positive value even when it should return 0), and therefore the integration term of the PI output grows without bounds. As a consequence, the laser falls out of lock. Despite what one might expect, a higher P-gain does not solve this problem.

The constant offset seems to be caused by a change in the relative intensity of the beams. Indeed, the relative intensity is extremely sensitive to changes in the angles of mirrors in the single and double beam preparation stages of the setup. An external perturbation might sometimes cause one of these angles to change slightly. Alternatively, the failure of the PI controller to respond to the high spike in the error signal at $t = 0.06$ ms could cause a constant offset afterwards, but the mechanism by which this may occur is unknown.

In the second type of unlock event, the laser does not experience any significant external perturbations. Instead, the PI output starts increasing or decreasing slowly without the error signal displaying significant spikes. The most likely explanation for

this behaviour (which occurs every 30 minutes to 1 hour) again is that the relative intensity of the beams changes over time, causing an offset in the frequency to which the laser is locked. If this offset gets too large, the error signal is no longer linear in the frequency detuning, so the laser unlocks. A slow change in relative intensity could occur because of thermal fluctuations causing mirrors to drift. Thus, improved temperature control inside the box housing the setup might at least partially alleviate this problem.

4.4 Width of Saturated Absorption Peak

For a large modulation frequency f_{mod}, the Doppler-free peaks of the two beams do not overlap, generating a difference signal such as the one shown in Fig. 4.5. Because the difference in frequency between the two peaks in the signal is known to be $2f_{\text{mod}}$, this distance can be used as a reference for the width of the Doppler-free peaks. Using this method, one obtains a full width at half maximum

$$f_{FWHM} \approx 6 \text{ Mhz}$$

for a typical Doppler-free peak. This width is not very sensitive to changes in beam alignment in the iodine cell or at the photodiode, so it is therefore likely to not be specific to this setup and stem largely from the natural line-width.

Indeed, a similar line-width of 10 ± 1.6 MHz was found by [9] for a hyperfine transition in the 568.2 nm line of molecular iodine. The line-width measured here and by [9] differ either be due to differences in the experimental setup or because different hyper-fine lines were considered.

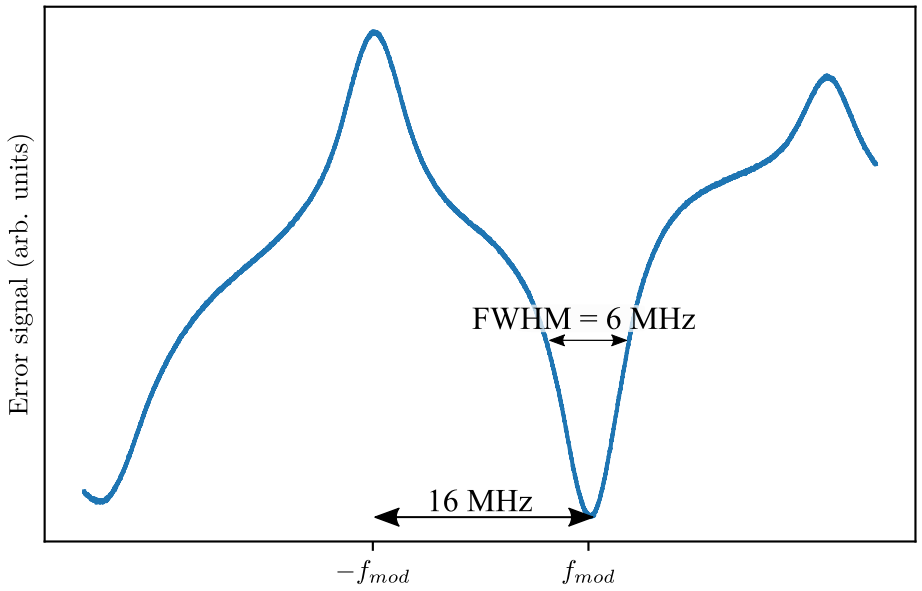

Figure 4.5: Error signal for $f_{\text{mod}} = 8$ Mhz (averaged over 128 periods). Because the modulation frequency is larger than the peak width, a distinct peak and dip are observed. By using the frequency difference between the two peaks as a reference, one obtains a linewidth of $f_{FWHM} = 6$ Mhz.

References

[1] C. J. Foot, *Atomic Physics*. Oxford University Press, Oxford, 2005.

[2] D. W. Preston, *Dopplerfree saturated absorption: Laser spectroscopy*, Am. J. Phys. **64**, 11 (1996) 1432–1436.

[3] H.-Y. Lo, *Creation of Squeezed Schrödinger's Cat States in a Mixed-Species Ion Trap*. DISS. ETH NO. 22902. 2015.

[4] D. T. X. Hung, *Laser frequency stabilization for optical trapping of Magnesium ions*. 2016.

[5] M. Aldous, J. Woods, A. Dragomir, R. Roy, and M. Himsworth, *Carrier frequency modulation of an acousto-optic modulator for laser stabilization*, `arXiv:1701.02181`.

[6] Personal conversations with Christoph Fischer.

[7] J. Home, *Physics III. Lecture Notes* (Version of Dec. 19, 2014).

[8] H. A. Radi and J. O. Rasmussen, *Principles of Physics*. Undergraduate Lecture Notes in Physics. Springer, Heidelberg, 2013.

[9] T. W. Hänsch, M. D. Levenson, and A. L. Schawlow, *Complete Hyperfine Structure of a Molecular Iodine Line*, Phys. Rev. Lett. **26**, 16 (1971) 946–949.

[10] B. M. Smirnov, *Principles of Statistical Physics*. Wiley-VCH, Weinheim, 2006.

[11] H. Tijms, *Understanding Probability*. Cambridge University Press, Cambridge, 2012.

[12] E. W. Weisstein, *Gaussian Function*. `http://mathworld.wolfram.com/GaussianFunction.html` [May 28, 2017].

A Mathematical Analysis of Doppler Broadening

Doppler broadening causes the spectral lines to assume the shape of a Gaussian, the functional form of which can be found from the Maxwell-Boltzmann-Distribution using the formula for the non-relativistic Doppler effect. The result will be used in appendix B to examine the absorption signal from two crossing beams.

In section A.1 we derive the probability density function for the z-component of the velocity of an iodine atom starting from the Maxwell-Boltzmann-Distribution using only elementary probability theory. The result is well-known from statistical mechanics (see [10, sections 2.5-2.7] for a derivation using the partition function).

A.1 Velocity Distribution of Iodine Atoms

We choose a coordinate system such that the z-axis is aligned with the direction of the laser beam used for spectroscopy. Consider an atom moving with velocity $\vec{v}$. Denote by θ the angle between the z-axis and $\vec{v}$ with $\theta \in [0, \pi)$. Then, the z-component of $\vec{v}$ is given by $v_z = v \cos\theta$ with $v = |\vec{v}|$. We assume that for atoms inside the iodine cell, the direction of the velocity vector is uniformly distributed. This assumption is justified as long as the momentum imparted by the photons in the pump beam on the iodine atoms is negligible compared to thermal motion, because the former always points in the z-direction whereas the latter is uniformly distributed. Under this assumption, the probability density function for θ is given by

$$P_\Theta(\theta) = \frac{1}{2}\sin(\theta)\,, \tag{A.1}$$

since an area element on a sphere scales with $\sin\theta$.

We are interested in the probability $P_{V_z}(v_z)dv_z$ that the z-component of the velocity of the atom under consideration has a value between v_z and $v_z + dv_z$. This is the case if and only if $\theta \in [\arccos\frac{v_z}{v}; \arccos\frac{v_z}{v} + d\theta]$. It follows:

$$\begin{aligned}
P_{V_z}(v_z|v)dv_z &= P_\Theta\left(\arccos\frac{v_z}{v}\right)d\theta \\
&= P_\Theta\left(\arccos\frac{v_z}{v}\right)\left|\frac{d\theta}{dv_z}\right|dv_z \\
&= \frac{1}{2}\sqrt{1+(v_z/v)^2}\left|\frac{d}{dv_z}\arccos\frac{v_z}{v}\right|dv_z \\
&= \frac{1}{2}\frac{\sqrt{v^2-v_z^2}}{v}\frac{1}{\sqrt{v^2-v_z^2}}dv_z \\
&= \frac{1}{2v}dv\,,
\end{aligned} \tag{A.2}$$

so the z-component of $\vec{v}$ is uniformly distributed between $-v$ and v. Therefore the probability density function (PDF) for v_z for an atom with a velocity v is given by

$$P_{V_z}(v_z|v) = \begin{cases} 1/(2v) & v_z \in [-v, v] \\ 0 & \text{otherwise} \end{cases}.$$

In probability theory, the above derivation is called a transformation of random variables. A more rigorous treatment can be found in [11, section 10.5].

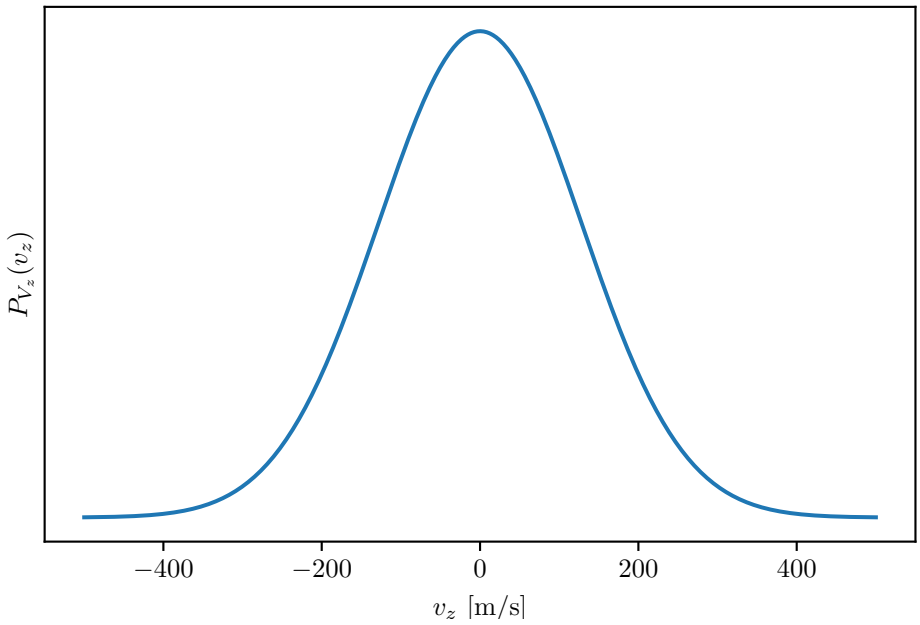

Figure A.1: Probability density function $P_{V_z}(v_z)$ for molecular iodine I_2 at 500 K.

The PDF of velocities v of the atoms in the iodine gas is given by the Maxwell-Boltzmann-distribution

$$P_M(v) = \sqrt{\frac{2}{\pi}} \frac{1}{\sigma^3} v^2 \exp\left(-\frac{v^2}{2\sigma^2}\right) , \tag{A.3}$$

where $\sigma = \sqrt{kT/m}$.

The probability density function of v_z for an atom with unknown velocity is then given by

$$P_{V_z}(v_z) = \int_{\mathbb{R}\setminus(-v_z,v_z)} P_M(v) P_{V_z}(v_z|v) dv \tag{A.4}$$

because $P_M(v)P_{V_z}(v_z|v)dvdv_z$ gives the probability of a particle having a speed in the interval $[v, v+dv]$ with a z-component of velocity in $[v_z, v_z+dv_z]$. Integrating over v means all possible values of v which satisfy $v_z \in [-v, v]$ are considered. Again, we refer to [11] (in particular chapter 13) for a more rigorous treatment.

The integral can be evaluated analytically using the substitution $u = v^2, du = 2vdv$ and yields

$$\begin{aligned} P_{V_z}(v_z) &= \int_{\mathbb{R}\setminus(-v_z,v_z)} \sqrt{\frac{1}{2\pi}} \frac{1}{\sigma^3} v \exp\left(-\frac{v^2}{2\sigma^2}\right) dv \\ &= \sqrt{\frac{1}{2\pi}} \frac{1}{\sigma} \exp\left(-\frac{v_z^2}{2\sigma^2}\right) , \end{aligned} \tag{A.5}$$

as shown in Fig. A.1 for iodine at 500 K.

A.2 Derivation of the Shape of Doppler Broadened Peaks

Let f_0 be the transition frequency of some molecule and f_L the frequency of the laser used to observe this transition. In the rest frame of a molecule with z-velocity v_z, the

laser moves with velocity $-v_z$ and thus has a frequency $f_D(v) = f_L\left(\frac{1}{1-v_z/c}\right)$, where we used the formula for the non-relativistic Doppler effect [8, eqn. 15.37], which is justified because from Fig. A.1 it is clear that the relevant velocities are non-relativistic. The condition for light to be absorbed is $f_D(v) = f_0$. This means that a molecule has to have velocity

$$v_z(f_L) = c(1 - f_L/f_0) \tag{A.6}$$

to be able to absorb light of frequency f_L. Therefore, the probability that an atom with given v_z absorbs light of frequency f_L is given by a δ-function

$$P_{\text{abs}}(f_L|v_z) = \delta(v_z - c(1 - f_L/f_0)) \tag{A.7}$$

as long as the natural linewidth is neglected.

With similar reasoning as for eqn. (A.4), we can now calculate the PDF for absorption using eqn. (A.7) and eqn. (A.5):

$$\begin{aligned} P_{\text{abs}}(f_L) &= \int P_{V_z}(v_z) P_{\text{abs}}(f_L|v_z) dv \\ &= \int \sqrt{\frac{1}{2\pi}} \frac{1}{\sigma} \exp\left(-\frac{v_z^2}{2\sigma^2}\right) \delta(v_z - c(1 - f_L/f_0)) dv \\ &= \sqrt{\frac{1}{2\pi}} \frac{1}{\sigma} \exp\left(-\frac{c^2(1 - f_L/f_0)^2}{2\sigma^2}\right) \\ &= \sqrt{\frac{1}{2\pi}} \frac{1}{\sigma} \exp\left(-\frac{c^2(f_0 - f_L)^2}{2f_0^2\sigma^2}\right) . \end{aligned} \tag{A.8}$$

The result is a Gaussian centered around f_0 with standard deviation $\sigma f_0/c$.

B Error Signal from Crossing Beams

It was observed experimentally that the error signal obtained from the difference between the saturated absorption spectra of two beams at frequencies $f \pm f_{\text{mod}}$ does not assume the desired form shown in Fig. 2.1 if the two beams cross each other inside the iodine cell. Here, a qualitative theoretical analysis of this situation is given. First, a simple model of saturated absorption spectroscopy is developed, which is then applied to the case of two crossing beams. Throughout this section, we will use notation introduced in appendix A.

B.1 Simple Model for Saturated Absorption Spectroscopy

For our model of saturated absorption spectroscopy, we make the following two assumptions:

1. The probe beam has no effect on the ground state population of molecules. This is justified as long as the probe beam is much weaker than the pump beam. In the setup with crossing beams, a neutral density filter was used which made the probe beam weaker by a factor of 10.

2. The number of absorbed photons from the pump and probe beam is proportional to the number of atoms in the velocity class capable of absorption. This means that the limiting factor for photon absorption is not the number of available photons, but the probability of a photon impinging on a suitable atom. This is justified because the intensity of the laser beam was observed to be high even after passing the iodine cell.

By assumption 1, the pump beam depletes the ground state population of the velocity class of molecules satisfying $v_z(f_L) \approx c(1 - f_L/f_0)$ (from (A.6)). Theoretically, only molecules satisfying eqn. (A.6) exactly will be depleted, yet it was observed experimentally that the Doppler-free peaks have a width of $f_{FWHM} \approx 6$ Mhz (section 4.4). This corresponds to a spread in velocities

$$\Delta v = 2c\frac{\Delta f}{f_0}$$

according to eqn. (A.6).

The factor 2 arises because for a given change in velocity, the frequency of both the pump and the probe beam changes. With $\Delta f = f_{FWHM}$ and $f_0 = 5.28 \cdot 10^{14}$ Hz (for the 568 nm line of iodine) one finds $v_{FWHM} = 7.8$ m/s. Therefore, the ground state depletion can be modeled using a Gaussian with standard deviation $\sigma_v = v_{FWHM}/\sqrt{8\log 2} \approx 2.9$ m/s [12]. Combining this with eqn. (A.5) and eqn. (A.6) yields:

$$P(v_z|f_L) = \underbrace{\left[1 - \gamma \exp\left(-\frac{(v_z - c(1 - f_L/f_0))^2}{2\sigma_v^2}\right)\right]}_{\text{Dip caused by pump beam with frequency } f_L} \underbrace{\left[\sqrt{\frac{1}{2\pi}}\frac{1}{\sigma}\exp\left(-\frac{v_z^2}{2\sigma^2}\right)\right]}_{\text{Underlying velocity distribution}}, \qquad \text{(B.1)}$$

where γ indicates the degree of saturation.

The probe beam travels opposite to the pump beam and thus is Doppler-shifted in the opposite direction. It is therefore clear from (A.6) that a probe beam with frequency

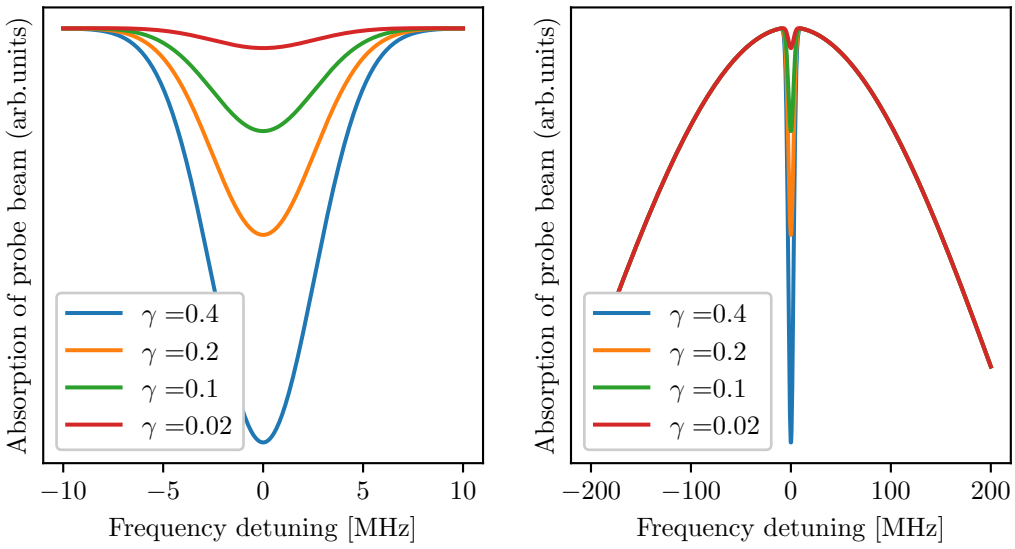

Figure B.1: Shape of the Doppler-free dip as predicted by theoretical model. The left figure shows the Gaussian of the Doppler-free dip, whereas the right figure shows the Doppler-free peak in the context of the Doppler dip. With higher saturation γ, the depth of the dip increases.

f_L is absorbed by molecules with velocity $v_z'(f_L) = c(f_L/f_0 - 1)$. Neglecting the natural linewidth of the probe beam absorption, we find the absorption curve for saturated absorption spectroscopy from (B.1):

$$\begin{aligned} A(f_L) &= P(c(f_L/f_0 - 1)|f_L) \\ &= \left[1 - \gamma \exp\left(-\frac{2c^2(f_L - f_0)^2}{f_0^2 \sigma_v^2}\right)\right] \left[\sqrt{\frac{1}{2\pi}}\frac{1}{\sigma} \exp\left(-\frac{c^2(f_L - f_0)^2}{2f_0^2\sigma^2}\right)\right]. \end{aligned} \tag{B.2}$$

Fig. B.1 shows this absorption spectrum and reproduces $f_{FWHM} = 6MHz$. $\gamma = 0.02$ most closely resembles the experimental data and will therefore be used from now on.

B.2 Application to Problem of Crossing Beams

The model developed in section B.1 can now be applied to the case of crossing beams. To do so, we need to modify the velocity distribution. In the region where beams of frequencies f_L^+ and f_L^- overlap, the two dips in the velocity distribution caused by each of the beams overlap. Therefore, (B.1) needs to be modified as follows:

$$\begin{aligned} P(v_z|f_L^+, f_L^-) = &\underbrace{\left[1 - \gamma \exp\left(-\frac{(v_z - c(1 - f_L^+/f_0))^2}{2\sigma_v^2}\right)\right]}_{\text{Dip caused by pump beam with frequency } f_L^+} \\ &\underbrace{\left[1 - \gamma \exp\left(-\frac{(v_z - c(1 - f_L^-/f_0))^2}{2\sigma_v^2}\right)\right]}_{\text{Dip caused by pump beam with frequency } f_L^-} \underbrace{\left[\sqrt{\frac{1}{2\pi}}\frac{1}{\sigma} \exp\left(-\frac{v_z^2}{2\sigma^2}\right)\right]}_{\text{Underlying velocity distribution}}. \end{aligned} \tag{B.3}$$

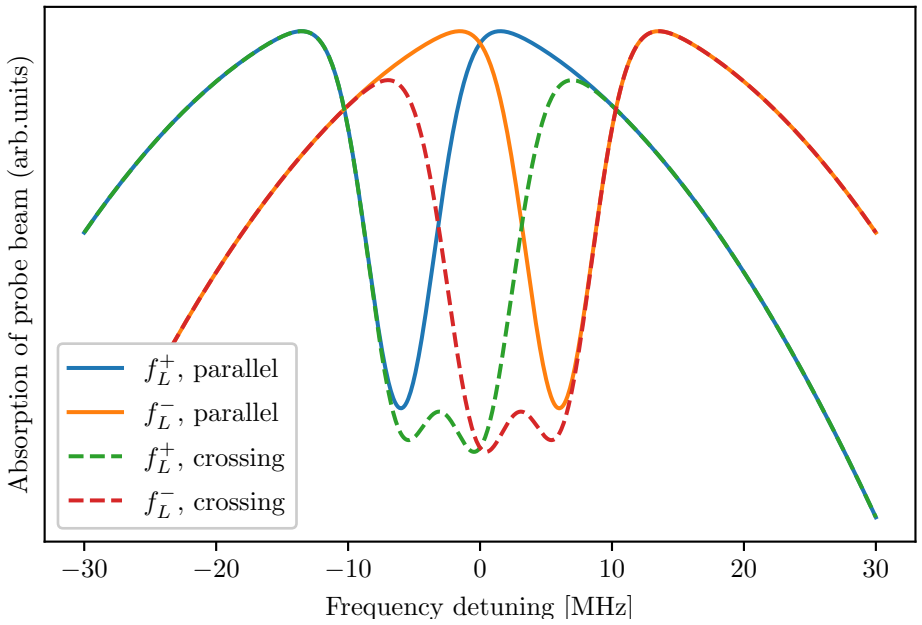

Figure B.2: Shape of the Doppler-free dips for both probe beams at frequencies $f_L^{\pm} = f_0 \pm 6$ MHz. The signal for both beams now displays two dips and is asymmetric.

By plugging $v_z^{\pm} = c(f_L^{\pm}/f_0 - 1)$ into this equation, we can obtain the shape of the saturated absorption spectrum for each probe beam individually:

$$P^{\pm}(f_L) = \left[1 - \gamma \exp\left(-\frac{2c^2(f_L^{\pm}/f_0 - 1)^2}{\sigma_v^2}\right)\right] \left[1 - \gamma \exp\left(-\frac{2c^2\left(\frac{f_L^+ + f_L^-}{2f_0} - 1\right)^2}{\sigma_v^2}\right)\right] \left[\sqrt{\frac{1}{2\pi}}\frac{1}{\sigma} \exp\left(-\frac{c^2(f_L^{\pm}/f_0 - 1)^2}{2\sigma^2}\right)\right], \quad \text{(B.4)}$$

where f_L^+ and f_L^- are understood to be functions of f_L. The result is shown in Fig. B.2.

We see that the signal for crossing beams is asymmetric and widened compared to the signal for parallel beams. This gives some intuition for why the error signal should degrade for two beams crossing, but the exact shape of the observed difference signal cannot be reproduced in this simple model.

C Recommended Settings for Current Setup

Modulation frequency	4 MHz
Modulation voltage	1 Vpp
AOM2 carrier frequency	110 MHz
AOM2 power	0 dBm
Photodiode setting	Balanced
P gain	15000
I gain	3

Table 1: Recommended settings for current setup.